Dual-active NiO-$Ce_{1-x}Ni_xO_2$ nanocomposite for catalytically upcycling PET into H_2

Jin Wang [1], Fangqi Liu [1], Chun Shan [1], Jiarui Zhu, Zengjian Guo, Xuesong Zhang [*], Lujia Han

Engineering Laboratory for AgroBiomass Recycling & Valorizing, College of Engineering, China Agricultural University, Beijing 100083, China

**Corresponding author, E-mail: xszhang@cau.edu.cn (X. Zhang)*

[1] These authors contributed equally to this article.

Supplementary

Experimental section

Materials

150-mesh polyethylene terephthalate (PET) powder was purchased from Huachuang Plastic Ltd., China. $Ni(NO_3)_2{\cdot}6H_2O$, $La(NO_3)_3{\cdot}6H_2O$, $Ce(NO_3)_3{\cdot}6H_2O$, $Sr(NO_3)_2$, citric acid, and other chemical reagents used for catalyst preparation were received from Beijing Keao Chemical Co., Ltd.

Catalyst synthesis

$ANiO_3$ (A = La, Ce, and Sr) perovskites were synthesized *via* the Pechini sol-gel method. A precursor solution was prepared by dissolving equimolar amounts of metallic nitrates with two equivalents of citric acid. The solution was then heated to 80 °C under continuous stirring (~300 rpm) until gelation was completed through water removal. To evaporate the excess water, the gel was transferred into an oven and dried at 160 °C for 4 h. Next, the powder was placed into an alumina crucible and calcined in two steps in a muffle furnace. The first step (450 °C for 2 h, ramping rate: 3 °C/min) combusted citric acid and decomposed the nitrates; the second step (held at 800 °C for 6 h, ramping rate: 5 °C/min) yielded the desired phases of perovskites. After calcination, the materials were naturally cooled to room temperature. The final catalysts were pressed and sieved to a particle size of approximately 20 - 40 mesh for catalytic steam reforming experiments with PET.

Catalytic steam reforming test

Similarly to our previous study, the catalytic steam reforming following non-catalytic thermal decomposition process (CSRD) was conducted employing a dual-stage reactor system (Fig. S1).[1] Moderate non-catalytic thermal decomposition of PET occurred in the upper stage, while the lower stage performed catalytic steam reforming. Prior to each experiment, 2.00 g of PET powder was preloaded in a quartz basket above the upper stage, and 1.00 g of catalyst was placed on the porous surface in the bottom stage. After checking the airtightness of the system, purge the system with argon (Ar) at a flow rate of 50 mL/min for 15 min to completely exclude the air. Subsequently, heat the upper and lower zones at 10 °C/min to 500 °C and 800 °C, respectively, maintaining for 10 min to stabilize the system. At the initiation of the reaction, water was injected into a steam generator at a rate of 36 mL/h, where it was immediately vaporized into steam to serve as the gasifying agent. Simultaneously, the quartz basket containing PET was inserted quickly into the upper stage and held for 20 min to facilitate rapid non-catalytic thermal decomposition of plastics, with the resulting products entering the lower stage for catalytic reforming. Throughout the reaction, maintain a continuous flow of Ar as the carrier gas at 50 mL/min. Condensable tar was captured by the condensing system, while non-condensable gases were collected for further analysis.

At the start of the reaction, water was injected into a steam generator at a rate of 36 mL/h, where it was immediately vaporized to serve as the gasifying agent. Simultaneously, the quartz basket containing PET was swiftly inserted into the upper

stage and held for 20 min to ensure rapid plastic non-catalytic thermal decomposition, with the resulting products directed into the lower stage for catalytic reforming. Throughout the reaction, Ar was continuously supplied as the carrier gas at 50 mL/min. Condensable tar was captured by the condensing unit, while non-condensable gases were collected for further analysis.

Catalyst characterization and in situ analysis

The crystalline phases of catalysts were investigated using the X-ray diffractometer (XRD, XD-3, Persee Ltd., Beijing, China). The X-ray photoelectron spectroscopy (XPS, ESCALAB 250Xi, ThermoFisher Scientific) was utilized to determine the surface chemical compositions of the catalysts. High-resolution transmission electron microscope (HRTEM, JEM-F200) was employed to further characterize the surface morphology of the carbonaceous catalysts. The elemental distribution was analyzed with the TEM equipped with energy-dispersive X-ray spectroscopy (EDS, JED-2300T). A temperature programmed oxidation (TPO) of spent catalysts was performed by using the thermogravimetric analyzer (SDT Q600, TA Instruments, USA) to determine coke deposition of the spent catalysts. *in situ* DRIFTS experiments were performed using a Bruker INVENIO S FTIR spectrometer equipped with a liquid-nitrogen cooled mercury-cadmium-telluride (MCT) detector and a Harrick Scientific HVC-DRP-4 reaction cell fitted with ZnSe windows. The background spectrum was collected under N_2 atmosphere at ambient temperature. The seven panels near the bottom represent the signal data collected at 30, 100, 200, 300, 400, and 500 °C

following the introduction of the experimental gas (5% mixed gas composed of CO and CH_4 in N_2 with water vapor). The five panels near the top represent the spectra of $CeNiO_3$ during the sequential introduction of experimental gas (2, 4, 6, 8, and 10 min) at 500 °C.

Shimadzu GC-2014 gas chromatography (GC, Shimadzu Corp., Kyoto, Japan) with a thermal conductivity detector (TCD) was used to identify and quantify all the gaseous products. A standard gas mixture (including H_2, CO, CH_4, and CO_2) was applied to calibrate the volumetric concentration (vol%) of gaseous fractions. The gas compositions ($\geqslant C_2$) were not observed or negligible in this study.

Data analysis

The mass of gaseous products was determined by correlating the total gas volume with the respective densities of individual gas components. Additionally, the char mass was assessed based on the solid residue remaining in the quartz basket. In this study, solid residues were observed after the CSRD process, likely due to the inherent stability of benzene rings in the feedstock. Consequently, carbon yield was included in the subsequent analysis.

The gas yield (Y_i, mmol/g_{PET}) represents the amount of gas *i*, in millimoles, generated per gram of PET:

$$Y_i\left(mmolg_{PET}^{-1}\right) = \frac{V}{22.4 \times m} \times x_i \quad (1)$$

Here, x_i (vol%) denotes the volume percentage of gas component i (such as H_2, CO, CH_4, and CO_2) measured by gas chromatography (GC); V (mL) represents the total volume of gas collected; and m (g) is the mass of plastic feedstock used in the CSRD process.

Carbon conversion efficiency was employed as a quantitative metric to evaluate the macromolecular restructuring of plastics within the CSRD process.

$$Carbon\ conversion\ efficiency\ = n \times \frac{12}{22.4} \times \frac{\sum V_i}{m_{PET} \times f_{C,PET}} \times 100\% \quad (2)$$

In this formulation, n corresponds to the carbon number, V_i represents the volume (L) of gaseous species i (i: CO, CH_4, and CO_2), m_{PET} designates the initial mass of raw PET, and f_c quantifies the fractional carbon content within raw PET.

Table S1. Oxygen species distribution based on XPS analysis.

	O_L	O_v	O_{surf}	O_{adv}
Proportion (%)				
Pristine $CeNiO_3$	63.35	10.34	10.82	15.49
Spent $CeNiO_3$	60.02	17.96	18.97	3.05

Table S2. Comparison of the representative studies and present work in terms of gas formation behaviors.

Feedstock	Technology	Reaction conditions				Gas product			Ref.
		Decomposition temperature (°C)	Catalytic temperature (°C)	Catalyst	Catalyst to feedstock ratio	Gas yield (mmol/g_{PET})	H_2 yield (mmol/g_{PET})	H_2 concentration (vol%)	
PET	Fixed bed	800	800	CaO	2:1	-	~16.20	-	2
PET	Fixed bed	700	700	10%Ni-1%Pd/Al_2O_3-La_2O_3	-	-	-	60.00	3
PET	One-pot	250	250	Ru-5ZnO	1:4	-	19.97	-	4
PET	Fixed bed	500	800	30NiO-CeO_2	1:2	-	27.60	-	5
PET	Fixed bed	500	800	$CeNiO_3$	1:2	98.21	54.58	55.56	This study

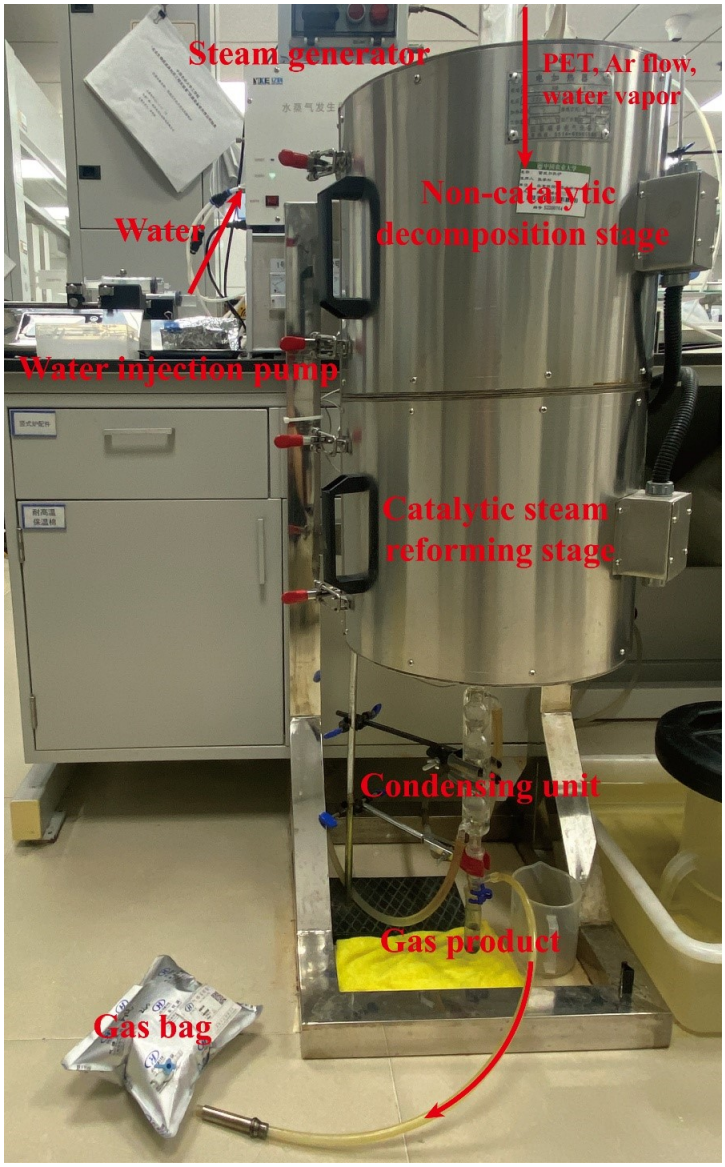

Figure S1. The experimental equipment and flowcharts.

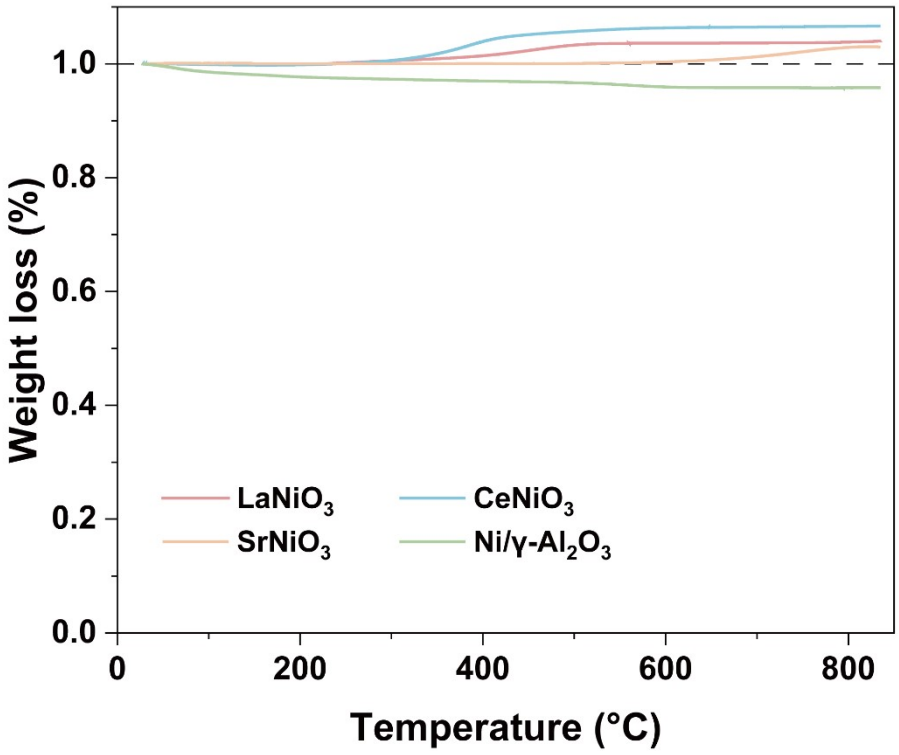

Figure S2. TPO profiles of the spent catalysts.

Notes and References

1. X. Zhang, G. Kong, Y. Jiang, L. Zhou, K. Wang, X. Zhang, G. Ji and L. Han, *One Earth*, 2024, **7**, 908-923.
2. S. Li, M. Inayat and M. Järvinen, *Appl. Energy*, 2023, **348**, 121536.
3. B. Nabgan, M. Tahir, T. A. T. Abdullah, W. Nabgan, Y. Gambo, R. Mat and I. Saeh, *Int. J. Hydrogen Energy*, 2017, **42**, 10708-10721.
4. H. Su, Y. Hu, H. Feng, L. Zhu and S. Wang, *ACS Sustainable Chem. Eng.*, 2022, **11**, 578-586.
5. C.-Y. Hsu, W.-T. Chung, T.-M. Lin, R.-X. Yang, S. S. Chen and K. C.-W. Wu, *Int. J. Hydrogen Energy*, 2024, **49**, 873-883.